


RESEARCH ARTICLE

Deoxyhypusine synthase, an essential enzyme for hypusine biosynthesis, is required for proper exocrine pancreas development

Leah R. Padgett¹ | Morgan A. Robertson² | Emily K. Anderson-Baucum¹ |
 Craig T. Connors² | Wenting Wu^{3,4} | Raghavendra G. Mirmira^{3,5,6,7} |
 Teresa L. Mastracci^{1,2,3,5} 

¹Indiana Biosciences Research Institute, Indianapolis, IN, USA

²Department of Biology, Indiana University-Purdue University-Indianapolis (IUPUI), Indianapolis, IN, USA

³Center for Diabetes and Metabolic Diseases, Indiana University School of Medicine, Indianapolis, IN, USA

⁴Department of Medical and Molecular Genetics, Indiana University School of Medicine, Indianapolis, IN, USA

⁵Department of Biochemistry and Molecular Biology, Indiana University School of Medicine, Indianapolis, IN, USA

⁶Department of Pediatrics, Indiana University School of Medicine, Indianapolis, IN, USA

⁷Kovler Diabetes Center and the Department of Medicine, University of Chicago, Chicago, IL, USA

Correspondence

Teresa L. Mastracci, Department of Biology, Indiana University-Purdue University-Indianapolis (IUPUI), 723 W. Michigan St., SL 306, Indianapolis, IN 46202 USA.
 Email: tmastrac@iu.edu

Funding information

Juvenile Diabetes Research Foundation International (JDRF), Grant/Award Number: 5-CDA-2016-194-A-N; HHS | NIH | National Institute of Diabetes and Digestive and Kidney Diseases (NIDDK), Grant/Award Number: 1R01DK121987-01A1

Abstract

Pancreatic diseases including diabetes and exocrine insufficiency would benefit from therapies that reverse cellular loss and/or restore cellular mass. The identification of molecular pathways that influence cellular growth is therefore critical for future therapeutic generation. Deoxyhypusine synthase (DHPS) is an enzyme that post-translationally modifies and activates the mRNA translation factor eukaryotic initiation factor 5A (eIF5A). Previous work demonstrated that the inhibition of DHPS impairs zebrafish exocrine pancreas development; however, the link between DHPS, eIF5A, and regulation of pancreatic organogenesis remains unknown. Herein we identified that the conditional deletion of either *Dhps* or *Eif5a* in the murine pancreas results in the absence of acinar cells. Because DHPS catalyzes the activation of eIF5A, we evaluated and uncovered a defect in mRNA translation concomitant with defective production of proteins that influence cellular development. Our studies reveal a heretofore unappreciated role for DHPS and eIF5A in the synthesis of proteins required for cellular development and function.

KEYWORDS

acinar cells, DHPS, eIF5A, exocrine pancreas, hypusine biosynthesis, mRNA translation, translational regulation

Abbreviations: CPA, carboxypeptidaseA; DHPS, deoxyhypusine synthase; E, embryonic day; eIF5A, eukaryotic initiation factor 5A; eIF5A^{HYP}, hypusinated form of eIF5A; ES, embryonic stem cells; GC7, N1-Guanyl-1,7-Diaminoheptane; Hypusine, hydroxyputrescine lysine; iPS, induced pluripotent stem; NOD, non-obese diabetic; P/M, polyribosome-to-monoribosome; R26R, ROSA26 reporter; TMT, tandem mass tag.

This is an open access article under the terms of the Creative Commons Attribution-NonCommercial License, which permits use, distribution and reproduction in any medium, provided the original work is properly cited and is not used for commercial purposes.

© 2021 The Authors. *The FASEB Journal* published by Wiley Periodicals LLC on behalf of Federation of American Societies for Experimental Biology.

1 | INTRODUCTION

Determining the mechanisms that direct organogenesis and cellular differentiation is key to understanding pathogenesis and designing treatments for disease. In particular, the generation of therapeutics for diseases characterized by cellular death and dysfunction would be significantly advanced with a greater understanding of the mechanisms that direct cell growth. As an example, elucidation of the transcriptional cascades that instruct pancreatic cell fate¹ has led to the development of in vitro cellular differentiation protocols involving the step-wise application of exogenous signals and cellular markers to generate insulin-producing beta cells from embryonic stem (ES) cells or induced pluripotent stem (iPS) cells in vitro.²⁻⁵ Given that diabetes is a chronic disease characterized by the destruction and/or dysfunction of the insulin-producing beta cells in the pancreas,⁶ application of these in vitro methods to generate beta cells for transplantation provides a promising avenue for the treatment of diabetes. Diseases of the exocrine pancreas including pancreatitis and exocrine insufficiency would also benefit from therapies that reverse cellular loss.^{7,8} Therefore, identifying mechanisms that can be exploited to stimulate the expression of digestive enzymes or factors that instruct acinar cell development and growth may provide a therapeutic avenue for these exocrine pancreas diseases.

Great strides have been made in understanding the transcriptional mechanisms that instruct cell fate in the pancreas; however, the role of mRNA translation in the regulation of pancreatic endocrine and exocrine cell development has largely been ignored. Eukaryotic translation initiation factor 5A (eIF5A) functions to facilitate mRNA translation, at the stages of initiation, elongation, and termination.⁹⁻¹¹ Interestingly, eIF5A is the only known protein to contain the unique polyamine-derived amino acid hypusine (hydroxyputrescine lysine).¹² The hypusinated form of eIF5A (eIF5A^{HYP}) is generated through a multi-step reaction, which is initiated by the enzyme deoxyhypusine synthase (DHPS) and uses the polyamine spermidine as a cofactor to modify the lysine at position 50 of eIF5A.¹³ eIF5A is highly conserved throughout evolution, including the amino acid sequence surrounding the hypusine residue, underscoring an important cellular function for this modification.¹⁴ Considering the evolutionary conservation of eIF5A, our lab previously investigated the role of the hypusine modification in pancreas development using the zebrafish model system. Both pharmacological inhibition (using N1-Guanyl-1,7-Diaminoheptane; GC7) and morpholino knockdown determined that DHPS was important for the differentiation of acinar cells.¹⁵ These findings in zebrafish confirmed a functional role for DHPS in the exocrine pancreas¹⁵; however, the mechanistic link between DHPS and the regulation of pancreatic organogenesis remained unknown. Previous studies demonstrated that both

Dhps and *Eif5a* were essential for murine development.^{16,17} Thus, the early embryonic lethality of these models precluded further study of organ development.

In this study, we used conditional allele approaches to decipher the requirement for hypusine biosynthesis in mammalian pancreas development. Our results determined that the conditional deletion of *Dhps* or its target eukaryotic initiation factor 5A (*Eif5a*) in the murine pancreas resulted a severe reduction in the exocrine pancreas. Given that DHPS catalyzes eIF5A hypusination,¹²⁻¹⁴ and the hypusinated form (eIF5A^{HYP}) functions in mRNA translation,⁹⁻¹¹ we evaluated and uncovered stalled translation elongation concomitant with the differential expression of proteins that influence exocrine pancreas growth and function. Taken together our findings indicate that acinar cell growth and function is regulated at the level of mRNA translation, and specifically that DHPS and eIF5A^{HYP} are required to instruct the synthesis of proteins needed for exocrine pancreas growth and function.

2 | MATERIALS AND METHODS

2.1 | Animal studies

Animals were maintained under protocols approved by the Indiana University School of Medicine Institutional Animal Care and Use Committee. Mice containing the *Dhps*^{LoxP} allele¹⁸ were bred with previously described mice harboring Cre recombinase under control of the mouse *Ptf1a* promoter (*Ptf1a-cre*)¹⁹ to generate DHPS mutants (*Dhps*^{LoxP/LoxP}; *Ptf1a-cre*, referred to as *Dhps*^{ΔPANC}) and littermate control animals. Mice were maintained on an outbred, mixed background. The *R26R*^{Tomato} reporter allele (B6.Cg-Gt(ROSA)26Sor^{tm14(CAG-tdTomato)Hze/J})²⁰ was bred into all mouse models to confirm Cre-mediated recombination. Timed matings were established and embryos harvested at embryonic day (E) 14.5 and 18.5. Noon on the day of appearance of a vaginal plug was considered E0.5. All embryos and adult animals were genotyped by PCR using primers previously described¹⁸⁻²⁰). For weaned animals, weight and blood glucose were measured using a digital scale (Fisher), and AlphaTrak2 glucose monitor and test strips (Fisher), respectively.

Mice containing the *Eif5a*^{LoxP} allele were also bred with the *Ptf1a-cre* and *R26R*^{Tomato} reporter allele to generate eIF5A mutants (*Eif5a*^{LoxP/LoxP}; *Ptf1a-cre*; *R26R*^{Tomato}, referred to as *Eif5a*^{ΔPANC}) and littermate control animals. Figure S1A includes a schematic for the construct design of the *Eif5a*^{LoxP} conditional allele. The following primers were used for genotyping the single loxP site in the *Eif5a*^{LoxP} allele: 5'-CCA CTT GTC CAC GTT TGT CC-3' (loxP forward) and 5'-CAA TGC CAA CCA GAT GGA CC-3' (loxP reverse), with expected PCR product sizes of 505 bp for the wildtype and

557 bp for the single loxP site. The following primers were used for genotyping the loxP site in the Neo cassette in the *Eif5a^{loxP}* allele: 5'-ATC CCT CCT CAG GCA TCT GGG-3' (Neo forward) and 5'-ATT ACC AGT CAG GCT TTG CCA CC-3' (Neo reverse), with expected PCR product sizes of 429 bp for the wildtype and 563 bp for the loxP site in the Neo cassette (Figure S1B).

2.2 | RNA in situ hybridization

RNA in situ hybridization was performed on 8 μ m tissue sections mounted on glass slides as previously described.²¹ Antisense riboprobes for *Eif5a*, *c-Myc*, and *Dhps* were transcribed from linearized plasmids (clone ID #3591197, #3962047, and #4240646, respectively; Thermo Scientific). RNA in situ hybridization was performed on pancreas tissue sections from E14.5 *Eif5a^{ΔPANC}* and littermate control embryos as well as E14.5 wildtype embryos. Sections were counterstained with nuclear fast red and imaged using a Nikon Eclipse 90i microscope (Nikon).

2.3 | Immunofluorescence and morphometric analysis

Embryos or adult tissues were harvested at the appropriate ages and fixed in 4% paraformaldehyde (Fisher Scientific), cryo-preserved using 30% sucrose, embedded in OCT (Fisher Scientific), and tissue sectioned onto glass slides. Methods previously described for embryo and pancreas tissue preservation and immunofluorescence were followed.²² Tissue sections (8 μ m) were stained using the following primary antibodies: guinea pig anti-insulin (DAKO; 1:500), rabbit anti-glucagon (1:500; 2760S, Cell Signaling Technology), goat anti-ghrelin (1:800; sc-10368, Santa Cruz), goat anti-carboxypeptidaseA (1:500; AF2765, R & D Systems); rabbit anti-amylase (1:500; A8273, MilliporeSigma); rabbit anti-HistoneH3^{PHOS} (1:250; #9701, Cell Signaling Technology), rabbit anti-Sox9 (1:500; AB5535; MilliporeSigma). Secondary antibodies including Alexa-488, Cy3, or Alexa-647 (Jackson ImmunoResearch) were used, followed by DAPI staining (Sigma) to visualize nuclei. Images were acquired with a 710 confocal microscope (Zeiss).

Morphometric analysis was performed by immunostaining every 10th section throughout the pancreas of each embryo. Quantification of individual hormone-expressing cells was performed at E14.5, and cell number was quantified versus total pancreas area as defined by carboxypeptidaseA (CPA)-expressing cells. For quantification of exocrine pancreas area at E18.5, area was defined by amylase-expressing cells. For both E14.5 and E18.5 analyses, pancreas tissue

area was calculated using ImageJ software. A Student's *t*-test was performed to determine statistical significance (Prism7, GraphPad).

2.4 | Puromycin incorporation assays

Pancreata were harvested from E14.5 embryos, placed into a 12-well plate containing cold RPMI 1640 media (Fisher) supplemented with 10% FBS (SH3091003, HyClone) and incubated at 37°C for 30 minutes. Puromycin (P8833, MilliporeSigma) was added at a final concentration of 20 μ g/mL and the samples were incubated for 20 minutes at 37°C. Following incubation, each explant was washed twice with 1 mL of ice-cold PBS containing 100 μ g/mL cycloheximide and snap frozen. Total pancreata were lysed in 30 μ L of lysis buffer and processed as described below for Western blot analysis. Puromycin incorporation was normalized to expression of the loading control ERK1/2.

2.5 | Western blot analysis

Whole pancreata were lysed in buffer containing 50 mM Tris, pH 8.0, 150 mM NaCl, 0.05% Deoxycholate, 0.1% IGEPAL CA-630, 0.1% SDS, 0.2% sarcosyl, 10% glycerol, 1 mM DTT, 1 mM EDTA, 10 mM NaF, protease inhibitors (Roche, # 11836170001), phosphatase inhibitors (Roche, #4906845001), 2 mM MgCl₂, 0.05% v/v Benzonase, and subjected to protein quantification using the DC Protein Assay Kit II (Bio-Rad, #5000112). Protein was separated by SDS-PAGE (4%-20% gel) and transferred onto PVDF membranes. The membranes were incubated with either a loading control or Revert (LI-COR Biosciences, #926-11016) for total protein quantitation. Membranes were blocked in Odyssey Blocking Buffer (LI-COR Biosciences, #927-40100) at room temperature for 1 hour, followed by incubation with primary antibodies at 4°C overnight. After washing with PBST buffer three times, blots were incubated with secondary antibodies for 1 hour. Antibodies were used at the following dilutions: anti-DHPS (1:2000; sc-365077, Santa Cruz); anti-eIF5A^{HYP} (1:2000; 23); anti-eIF5A^{TOTAL} (1:2000; BDB611977 Clone 26 BD, Biosciences); anti-Pancreatic Lipase (1:2000; ABS547MI, MilliporeSigma); anti-Elastase (1:2000; ab68672, Abcam); anti-Carboxypeptidase (1:2000; AF2765, R & D Systems); anti-Amylase (1:2000; A8273, MilliporeSigma); anti-Puromycin (1:2000; MABE341, MilliporeSigma); anti-ERK1/2 (1:2000; #9102S, Cell Signaling Technology); anti-PDX1 (1:2000; ab47383, Abcam); anti-HistoneH3^{PHOS} (1:2000; #9701S, Cell Signaling Technology); and anti-HistoneH3 (1:2000; #50-193-303, Cell Signaling Technology). Immunoblots were visualized using fluorescently labeled secondary antibodies

(LI-COR Biosciences) and quantified using Image Studio Software (LI-COR Biosciences). Statistical significance was determined by a Student's *t*-test (Prism7, GraphPad).

2.6 | Ribosome profiling

Ribosome profiling experiments were performed as described previously.²⁴ In brief, cell lysate, from pancreas tissue dissected from E14.5 embryos, was passed through a 10-50% sucrose gradient and fractionated using a piston gradient fractionator (Biocomp Instruments). Absorbance at 254 nm was recorded using an in-line UV monitor (Biocomp Instruments). Polyribosome-to-monoribosome (P/M) ratios were quantitated by calculating the area under the curve corresponding to the polyribosome peaks (more than two ribosomes) divided by the area under the curve for the monoribosome (80S) peak; a Student's *t*-test was performed to determine statistical significance (Prism7, GraphPad).

2.7 | Quantitative proteomics

Whole pancreata dissected from E18.5 embryos were homogenized in 8 M urea in 50 mM Tris-HCL followed by sonication and a 2-hour incubation at room temperature. Protein concentration for each sample was quantified using the Bio-Rad protein assay (#5000001; Bio-Rad Laboratories). For each sample, equal amounts of protein (30 μ g) was reduced with 5 mM tris(2-carboxyethyl) phosphine hydrochloride (TCEP) and alkylated with 10 mM chloroacetamide (CAM) followed by overnight digestion with trypsin/LysC mix (Promega). Digested samples were cleaned up using a Sep-Pak C18 purification system (Waters).

For tandem mass tag (TMT) labeling, digested peptides from each sample were labeled with different isobaric TMT tags using the Thermo Fisher Scientific 11-plex TMT kit per manufacturer's instructions. Following individual labeling, peptide concentration was measured using the Pierce Quantitative Colorimetric Peptide Assay Kit (ThermoScientific), and equal sample amounts were mixed. To improve sequence coverage and detection, the mixed samples were fractionated using Pierce High pH Reverse-Phase Peptide Fractionation Kit (ThermoScientific). Samples were dried using a vacuum centrifuge and resuspended in 0.1% formic acid prior to LC-MS analysis.

For HPLC and mass spectrometry analysis, 10 μ L of each sample was loaded onto an Acclaim PepMap C18 trapping column (3 μ m particle size, 100 \AA pore size, 2 cm length, and 75 μ m outer diameter) and eluted onto a PepMap RSLC C18 column (2 μ m particle size, 100 \AA pore size, 25 cm length, and 75 μ m outer diameter) with a linear gradient from 3% to 35% acetonitrile (in water with 0.1% formic acid) over

180 minutes in-line with an Orbitrap Fusion Lumos Mass Spectrometer (Thermo Fisher Scientific). Raw files generated from the run were analyzed using Thermo Proteome Discoverer (PD) 2.2 SEQUEST HT (as a node in PD 2.2) as previously described.²⁵ The spectral false discovery rate (FDR) was set to $\leq 1\%$ as previously described.²⁶ The mouse FASTA sequences used for alignment were downloaded January 9, 2017 from Uniprot and included the addition of 72 common contaminants. The TMT total intensity value used for comparing abundances of individual proteins was derived from the number of tryptic peptides that matched a known protein within the used database.

3 | RESULTS

3.1 | *Dhps* is essential for acinar cell development

To investigate the functional role of DHPS in mammalian pancreas development, we generated a mouse model where *Dhps* was conditionally deleted in the *Ptf1a*-expressing pancreatic progenitor cells (*Dhps*^{LoxP/LoxP}; *Ptf1a-cre*,^{18,19} hereafter referred to as *Dhps* ^{Δ PANC}). We also incorporated the *R26R*^{Tomato} reporter allele²⁰ to confirm Cre-mediated recombination. Western analysis was used to measure DHPS loss in the pancreas and the concomitant reduction in expression of eIF5A^{HYP} as a function of total eIF5A expression (Figure 1A,B).

Forty-seven different intercrosses produced 466 offspring including *Dhps* ^{Δ PANC} mutant mice and controls of all expected genotypes; Chi-square analysis determined the *Dhps* ^{Δ PANC} mutant mice were born at the expected Mendelian frequency ($\chi^2 = 3.5$; $P = .17$). After weaning (3 weeks of age), initial observations showed that the growth of the *Dhps* ^{Δ PANC} animals was impaired compared with littermate controls (Figure). Weaned litters were subsequently monitored weekly for general health, weight, and blood glucose. *Dhps* ^{Δ PANC} mice were active similar to littermate controls but were significantly reduced in weight, showed relative hypoglycemia, and died by 6 weeks of age (Figure 1C,D). Identical results were observed for both male and female mutant mice (Figure S2). Tissue analysis revealed a nearly absent pancreas in 4-week-old *Dhps* ^{Δ PANC} mice when compared with *Ptf1a-cre* control littermates; the remnant pancreas tissue expressed the *R26R*^{Tomato} reporter indicating these cells did not escape Cre-mediated deletion (Figure 2A). We performed immunofluorescence analyses to determine the cellular composition of the remaining *Dhps* ^{Δ PANC} tissue. Notably, islets were present in the *Dhps* ^{Δ PANC} mutant pancreatic remnant; insulin and glucagon staining confirmed the presence of beta and alpha cells, respectively, in these islets (Figure 2B). In contrast, there was a stark absence of carboxypeptidaseA (CPA)-expressing

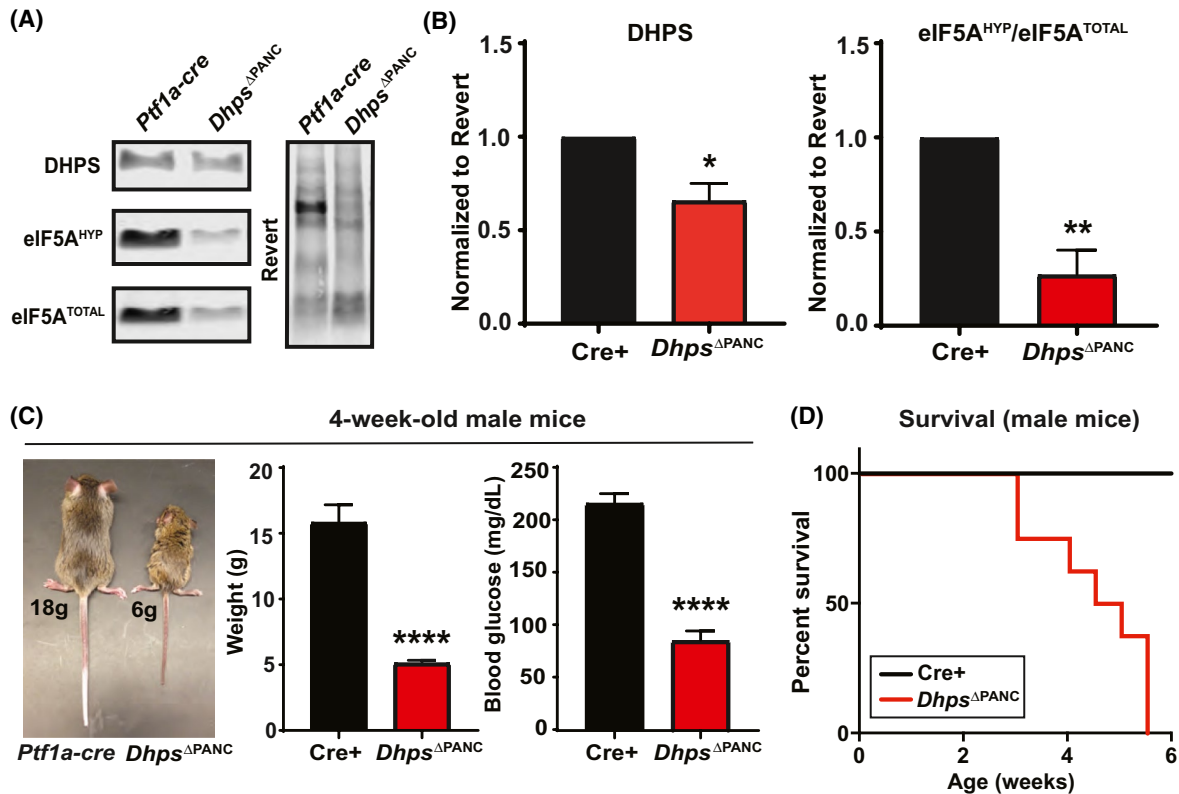


FIGURE 1 Deletion of pancreatic *Dhps* results in reduced whole-body growth and premature death. A, Western blot analysis of pancreata harvested from 3-week-old *Ptf1a-cre* (control) and *Dhps*^{ΔPANC} mice. B, Densitometry values were normalized to total protein input as detected by Revert. Relative protein expression levels are shown in the bar graphs. Data are presented as mean ± SEM, n = 3, *P < .05, **P < .005. C, Representative image, body weight, and blood glucose of male *Ptf1a-cre* (control) and *Dhps*^{ΔPANC} animals at 4 weeks of age. Data are presented as mean ± SEM, n = 8/group, ****P < .0001. D, Deletion of *Dhps* results in premature death by 6 weeks of age for male *Dhps*^{ΔPANC} animals. Similar results observed with female *Dhps*^{ΔPANC} mice (Figure S2)

cells, indicating a severe loss of exocrine tissue (Figure 2B). Western blot analysis confirmed a significant reduction in the expression of multiple digestive enzymes normally expressed in acinar cells including pancreatic lipase, elastase, CPA, and amylase (Figure 2C,D). Together, these data indicate that DHPS is dispensable for islet cell development and essential for acinar cell development.

3.2 | Pancreas size and endocrine cell populations are unchanged at embryonic day (E)14.5 in the absence of *Dhps*

Given the severe phenotype observed postnatally, we assessed pancreas development in *Dhps*^{ΔPANC} and *Ptf1a-cre* control embryos to determine when loss of DHPS function impacts pancreatic organogenesis. In particular, we characterized the pancreatic cell populations present at embryonic day (E)14.5, a stage during pancreas development known as the “secondary transition” and characterized by significant pancreatic growth and endocrine and exocrine cell differentiation.¹ DHPS and eIF5A are ubiquitously expressed in the developing embryo¹⁷; however, we confirmed that *Dhps*

and *Eif5a* gene expressions were specifically present in the pancreas at this critical stage of development. Using immunofluorescence and in situ hybridization on adjacent serial sections of E14.5 embryonic pancreas, we observed expression of both genes in the pancreatic ductal epithelium and CPA+ cells (Figure S3). These data demonstrate that DHPS and eIF5A are expressed in the cells that become both endocrine and exocrine.

By gross examination, there were no overt differences in pancreas structure at E14.5 (Figure 3A). Using immunofluorescence staining for CPA-expressing cells, which demarcate “tip” cells,²⁷ we quantified pancreas area and determined there was no statistically significant difference in the average pancreas size between the *Dhps*^{ΔPANC} and *Ptf1a-cre* controls (Figure 3B). Moreover, morphometric analysis of the endocrine cell populations present in the pancreas at E14.5, including insulin-expressing beta cells, glucagon-expressing alpha cells, ghrelin-expressing epsilon cells, and glucagon/ghrelin co-expressing cells, identified no statistically significant difference in cell numbers in the *Dhps*^{ΔPANC} compared with *Ptf1a-cre* controls (Figure 3C-H). Additionally, we quantified cells expressing phosphorylated histone H3 (PHH3), a marker of proliferation, and

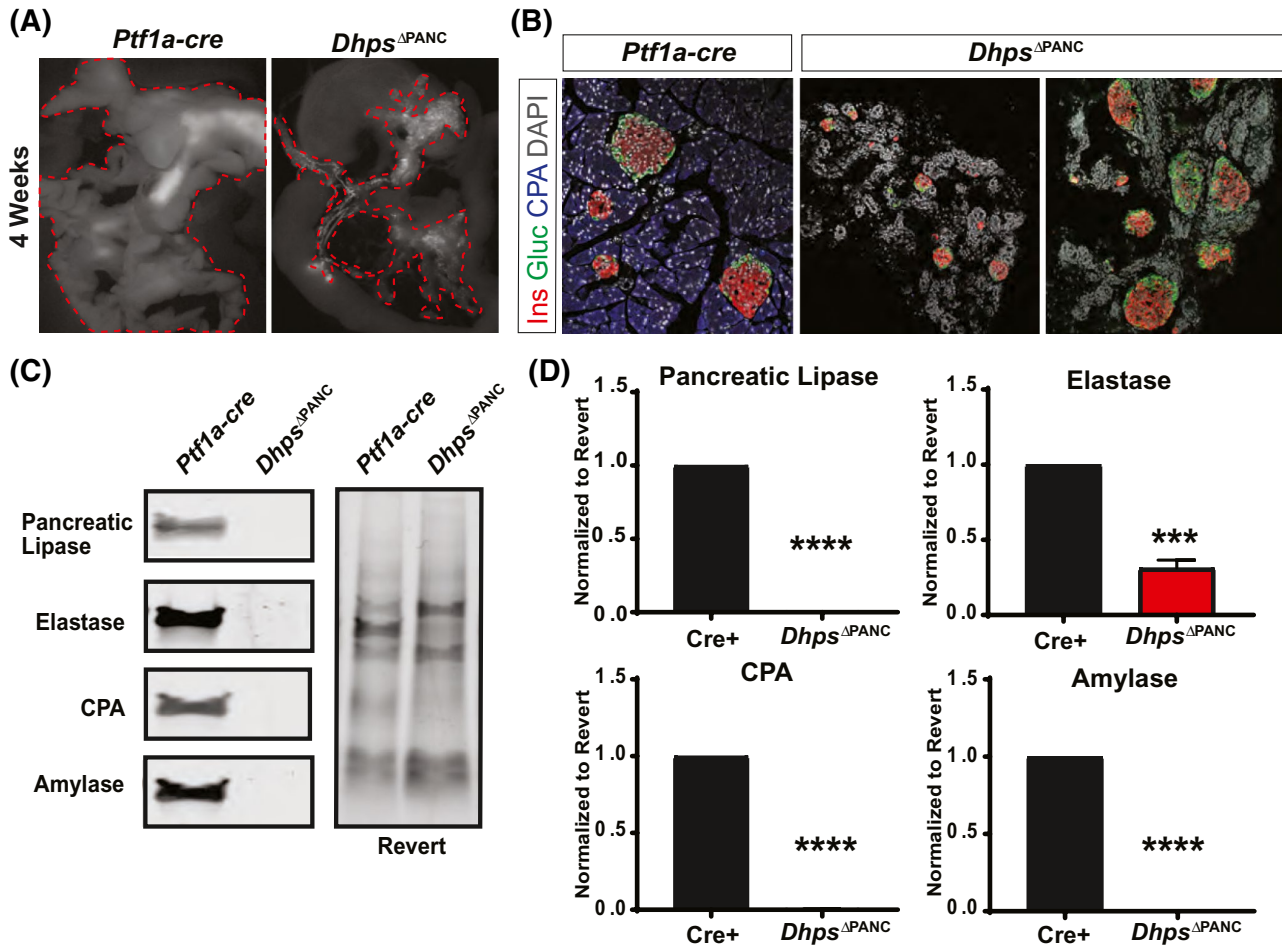


FIGURE 2 Deletion of pancreatic *Dhps* results in a near complete absence of exocrine tissue. A, Representative image of pancreata from *Ptf1a-cre* (control) and *Dhps*^{ΔPANC} mice at 4 weeks (dotted red lines encircle the grey-scale image of the *R26R^{Tomato}* reporter expression in the pancreas). B, Pancreatic tissue from 5-week-old *Ptf1a-cre* (control) and *Dhps*^{ΔPANC} mice analyzed by immunofluorescence for expression of the islet hormones insulin (Ins; red); glucagon (Gluc; green) and the exocrine enzyme carboxypeptidaseA (CPA; blue); cell nuclei are stained with DAPI (grey). Two representative images are shown for the *Dhps*^{ΔPANC} tissue. C, Western blot analysis performed on pancreata harvested from 3-week-old control and *Dhps*^{ΔPANC} mice. D, Densitometry values were normalized to total protein input as detected by Revert staining. Relative protein expression levels are shown in the bar graphs. Data are mean \pm SEM, $n = 3$, *** $P < .001$, **** $P < .0001$

determined there was no difference between the mutants and controls (Figure 3I-K). Collectively these data indicate that the deletion of *Dhps* from the earliest pancreatic progenitor cells expressing *Ptf1a* (at E9.5) does not influence cell differentiation before E14.5. Furthermore, our data suggest that the severe loss of exocrine pancreas observed in the postnatal setting was not because of missing cell types in early embryonic pancreas development.

To determine if the phenotype observed in the postnatal *Dhps*^{ΔPANC} mutants resulted from loss of the hypusinated form of eIF5A (eIF5A^{HYP}) or if eIF5A plays a role in pancreas development outside of that contributed by eIF5A^{HYP}, we generated a conditional allele for *Eif5a* (*Eif5a*^{LoxP}) wherein exons 4 to 7 of the *Eif5a* gene were flanked by Cre recombinase recognition sites (LoxP) (Figure S1). The *Eif5a*^{LoxP} mice were then crossed with *Ptf1a-cre* mice¹⁹ to generate a mutant mouse (*Eif5a*^{LoxP/LoxP}; *Ptf1a-cre*, hereafter referred to as *Eif5a*^{ΔPANC}) with a deletion of *Eif5a* in the

Ptf1a-expressing pancreatic progenitor cells. PCR genotyping and in situ hybridization were performed to confirm *Eif5a* deletion in the pancreas (Figure S1B,C). Akin to the *Dhps*^{ΔPANC} mice, we assessed pancreas size (Figure 4A-C) and the presence of endocrine and duct cell populations (Figure 4D-L) at E14.5 in the *Eif5a*^{ΔPANC} animals compared with *Ptf1a-cre* controls. This morphometric analysis of *Eif5a*^{ΔPANC} and *Ptf1a-cre* control animals revealed no significant difference in pancreas area as defined by CPA-expressing cells, and no difference in beta cell, alpha cell, ghrelin cell, and glucagon/ghrelin co-expressing cell numbers, as well as no alteration in the amount or arrangement of the Sox9-expressing ductal epithelium. These data confirm that the deletion of either *Dhps* or *Eif5a* from the *Ptf1a*-expressing pancreatic progenitor cells does not alter pancreatic development before E14.5 or initiation of the secondary transition, a critical stage for endocrine and exocrine cell differentiation.

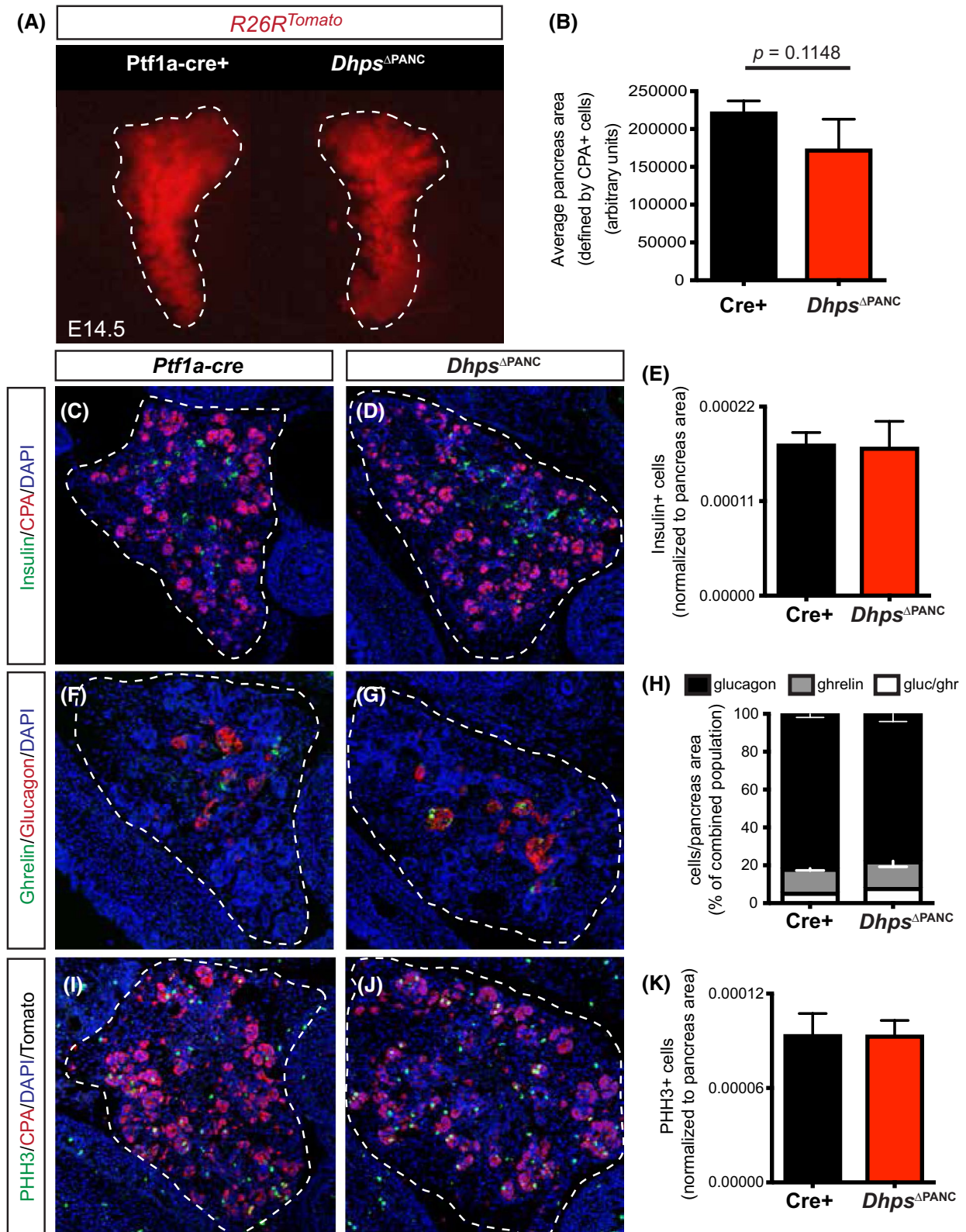


FIGURE 3 In the absence of *Dhps*, pancreas size and endocrine cell populations are unchanged during the secondary transition. A, Representative wholemount image of *Ptf1a-cre* (control) and *Dhps^{ΔPANC}* pancreata at embryonic day (E) 14.5 (dotted lines encircle tomato (red)-expressing pancreata). Pancreatic morphology was evaluated and appeared visually identical between *Dhps^{ΔPANC}* mutants and controls. B, Immunofluorescence for carboxypeptidaseA (CPA) was used to quantify pancreas area at E14.5 and showed no significant difference between mutants and controls ($n = 4/\text{group}$). Pancreas tissue sections were also evaluated for the expression of (C-E) insulin, (F-H) glucagon and ghrelin; cell nuclei are stained with DAPI (blue). Quantification of endocrine cell types showed no significant difference in cell numbers between *Dhps^{ΔPANC}* mutants and controls. I-K, E14.5 pancreas tissue was also analyzed for changes in proliferation using expression of phosphorylated histone H3 (PHH3); no difference was observed. Dotted lines demark the pancreas ($n = 4/\text{group}$). Data are presented as mean \pm SEM

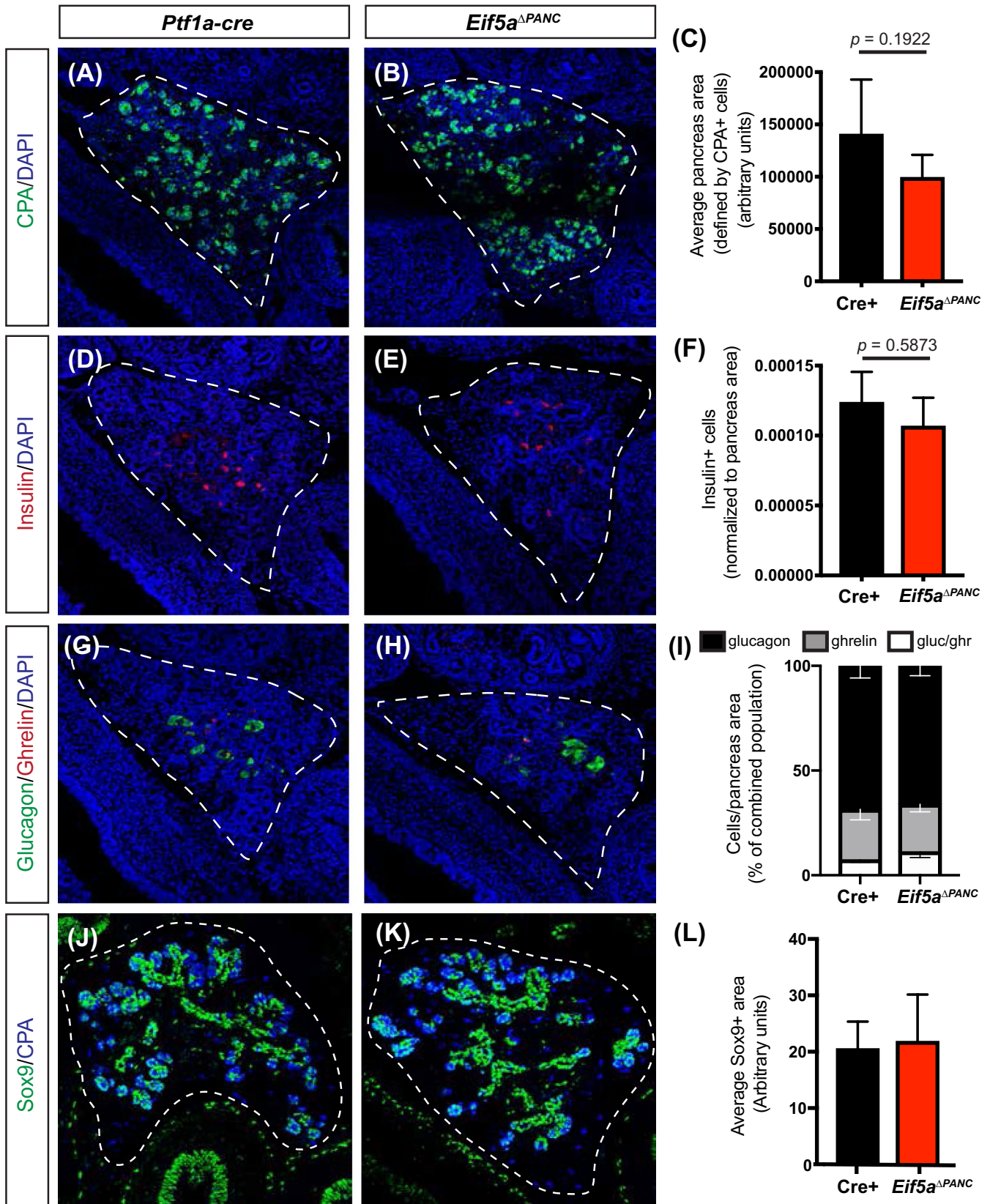


FIGURE 4 Loss of *Eif5a* in the pancreas does not alter pancreas size and endocrine cell specification at E14.5. A-C, Using immunofluorescence for carboxypeptidase A (CPA), pancreas area was quantified at E14.5 in *Ptf1a-cre* (control) and *Eif5a*^{ΔPANC} mutants; no significant difference was observed ($n = 4/\text{group}$). Pancreas tissue sections were also evaluated for the expression of (D-F) insulin, (G-I) glucagon and ghrelin, and (J-L) Sox9. Quantification identified no significant difference in endocrine cell numbers and Sox9+ ductal cell area between *Eif5a*^{ΔPANC} mutants and *Ptf1a-cre* controls. Cell nuclei were stained with DAPI. Dotted lines demark the pancreas ($n = 4/\text{group}$). Data are presented as mean \pm SEM

3.3 | Pancreas deletion of *Dhps* alters mRNA translation

Given the lack of changes in the pancreas of *Dhps*^{ΔPANC} mutants observed by morphometric analysis at E14.5, we confirmed by immunoblot that expression of DHPS was in fact significantly reduced in *Dhps*^{ΔPANC} mutant pancreata at this time point (Figure 5A,B). These results were in line with our findings from the immunoblot analysis of postnatal pancreas tissue (Figure 1A,B). Therefore, we hypothesized that the unaltered appearance of pancreas development at E14.5 but lack

of exocrine tissue in *Dhps*^{ΔPANC} adult mice may result from disrupted mRNA translation in the developing acinar cells during pancreatic organogenesis. To investigate the function of DHPS in mRNA translation in the pancreas, we used ribosome profiling. This technique uses a sucrose gradient to separate mRNA-ribosome complexes based on the number of associated ribosomes. Litters of E14.5 embryos were dissected for pancreata, which were subsequently treated with cycloheximide to stabilize the mRNA-ribosome complexes in situ; this lysate was centrifuged through a sucrose gradient to separate the transcripts based on the rate of sedimentation. The

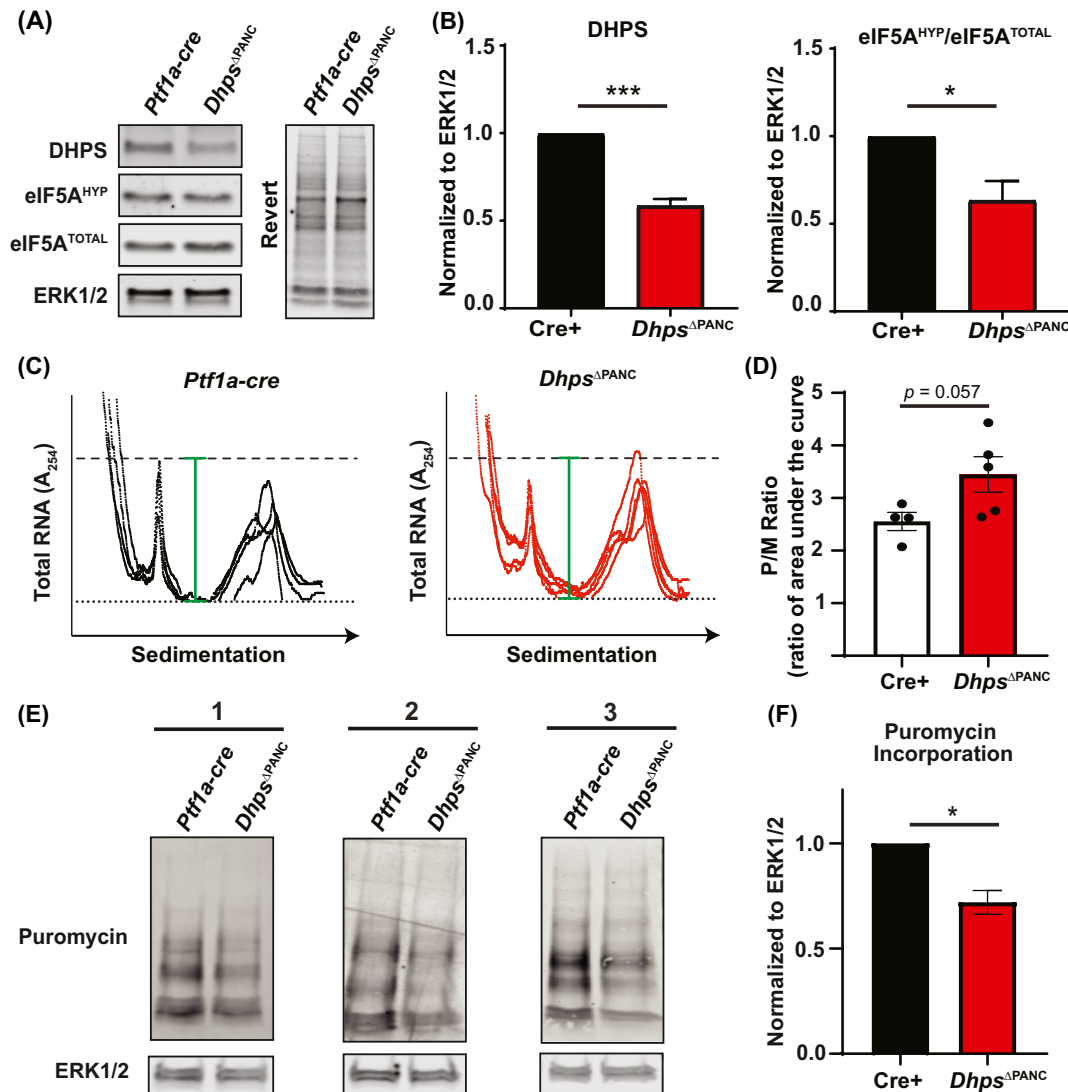


FIGURE 5 Pancreas deletion of *Dhps* alters mRNA translation. A, Western blot analysis of E14.5 pancreata harvested from *Ptf1a-cre* (control) and *Dhps*^{ΔPANC} mice. B, Densitometry values were normalized to the loading control ERK1/2 and relative protein expression levels are shown. Data are presented as mean ± SEM, n = 3, *P < .05, ***P < .0005. C, Ribosome profiling traces from E14.5 *Ptf1a-cre* (control) and *Dhps*^{ΔPANC} pancreata (n = 4-5/group). Horizontal dotted line demarks the baseline. Horizontal dashed line demarks the top of the mono-ribosome peaks in the control, which is then copied on to the mutant trace; green vertical lines demonstrate the distance from the baseline to the top of the mono-ribosome peaks of the controls. D, Quantification of the poly-ribosome to mono-ribosome (P/M) area under the curve. Data represented as mean ± SEM; black dots represent individual samples. E, Western blot analyses of E14.5 *Ptf1a-cre* (control) and *Dhps*^{ΔPANC} pancreata to assess protein synthesis by puromycin incorporation. Three independent experiments shown. F, Puromycin densitometry values were normalized to the loading control ERK1/2. Relative protein expression shown in the bar graph; data are presented as mean ± SEM, n = 3/group, *P < .05

abundance of mRNAs in the monoribosome and polyribosome fractions was quantified. Compared with *Ptf1a-cre* control pancreata, *Dhps*^{ΔPANC} ribosome profiles showed a decrease in the monoribosome fractions and an increase in the polyribosome fractions. Quantification of the monoribosome and polyribosome area under the curve for each sample showed an increased polyribosome to monoribosome (P/M) ratio (Figure 5C,D).

In general, an observed increase in the polyribosome fraction can indicate either (a) an increased rate of mRNA translation or (b) stalling of ribosomes on the mRNAs; stalled ribosomes would lead to a block in mRNA translation elongation and a build-up of transcripts in the polyribosome fraction. To determine the correct interpretation, we used puromycin incorporation to quantify total protein synthesis in the pancreas in the absence of *Dhps*. Pancreata were again harvested from control and *Dhps*^{ΔPANC} E14.5 embryos, and then treated with puromycin, a tyrosyl-tRNA analog that actively incorporates into nascent polypeptide chains. Western blot analysis revealed reduced puromycin incorporation and thus, reduced protein synthesis in the *Dhps*^{ΔPANC} pancreata compared with *Ptf1a-cre* controls (Figure 5E,F). Collectively, the reduced protein synthesis as determined by puromycin incorporation and increased P/M ratio from the ribosome profiling of *Dhps*^{ΔPANC} pancreata suggests that loss of *Dhps* results in a block in mRNA translation elongation.

3.4 | Proteins required for exocrine development and function are differentially expressed in the absence of hypusine biosynthesis

Tissue analysis revealed only a remnant remained of the exocrine pancreas, but the pancreatic islets were present in 4-week-old *Dhps*^{ΔPANC} mice when compared with control littermates (Figure 2), indicating loss of hypusine biosynthesis more significantly impacted exocrine pancreas development. Moreover, despite the lack of morphological phenotype at E14.5 (Figure 3), we did detect alterations in mRNA translation and reduced protein synthesis in the pancreas of *Dhps*^{ΔPANC} mutants at this embryonic stage (Figure 5). These findings thus prompted our investigation of the protein changes at E18.5, a later timepoint during pancreas development wherein more extensive exocrine development has occurred. Previous studies have shown that eIF5A^{HYP} has a half-life of seven days or longer,²⁸⁻³⁰ suggesting that the molecular effects of *Dhps* loss may only start to emerge at E14.5 and may appear more prominent at E18.5. To investigate the effect of *Dhps* on pancreatic development at this later timepoint, we harvested pancreata from E18.5 control, *Dhps*^{ΔPANC} and *Eif5a*^{ΔPANC} embryos to allow for a comparison of the proteins changed in the absence of either DHPS or eIF5A. Compared with *Ptf1a-cre* controls (the Cre

driver used to generate both mutant mouse models), western blot analysis confirmed decreased expression of DHPS in the *Dhps*^{ΔPANC} mutant, decreased expression of eIF5A^{TOTAL} in the *Eif5a*^{ΔPANC} mutant, and decreased expression of eIF5A^{HYP} in both mutants (Figure 6A,B). At E18.5, morphometric analysis confirmed that exocrine tissue was significantly reduced in size but not absent in either the *Dhps*^{ΔPANC} or *Eif5a*^{ΔPANC} mutants (Figure S4), and the remaining tissue showed decreased expression of the digestive enzymes CPA and Elastase as well as the transcription factor Pdx1 (Figure 6A,B). These data confirm that digestive enzymes, which characterize differentiated acinar cells,²⁷ as well as a transcription factor critical for pancreas development³¹ were significantly reduced with genetic loss of hypusine biosynthesis in the embryonic pancreas; however, these three proteins alone do not explain the dramatic phenotype observed in the pancreas of adult mutants.

To determine in an unbiased manner the proteins altered in the absence of either *Dhps* or *Eif5a*, we used quantitative proteomic analysis. Overall, this analysis detected 4645 proteins. The comparison of pancreata from *Ptf1a-cre* controls and *Dhps*^{ΔPANC} mutants identified 38 significantly differentially expressed proteins ($P < .05$; fold change > 1.5), both up- and down-regulated (Figure 6C). Comparison of pancreata from the *Ptf1a-cre* controls and *Eif5a*^{ΔPANC} mutants identified 49 significantly differentially expressed proteins ($P < .05$; fold change > 1.5) (Figure 6D). Interestingly, comparison of these lists of differentially expressed proteins identified 28 proteins co-altered in the *Dhps*^{ΔPANC} and *Eif5a*^{ΔPANC} mutant pancreata, with most of these proteins being digestive enzymes or proteins that influence cellular development (Figure 6E).

4 | DISCUSSION

For diseases characterized by cellular death and dysfunction, determining the mechanisms that direct organogenesis and cellular differentiation are critical to the generation of therapeutics. In particular, diseases of the pancreas, such as diabetes, pancreatitis, and exocrine insufficiency, would benefit from therapies that reverse cellular loss and restore the expression of missing hormones or digestive enzymes. With respect to diabetes, beta cell replacement or regeneration would be a landmark advance as these therapies would resolve the insulin imbalance and restore an individual's ability to respond to metabolic cues. To that end, the in vitro differentiation of beta cells for therapeutic transplantation is slowly being realized; however, cellular or regenerative therapies for diseases of the exocrine pancreas are not as well defined. Surgery, diet modification, and pharmaceutical treatments to resolve pain and replace digestive enzymes are standard of care for individuals suffering from pancreatitis or exocrine insufficiency^{7,32}; however, regenerating functional acinar cells

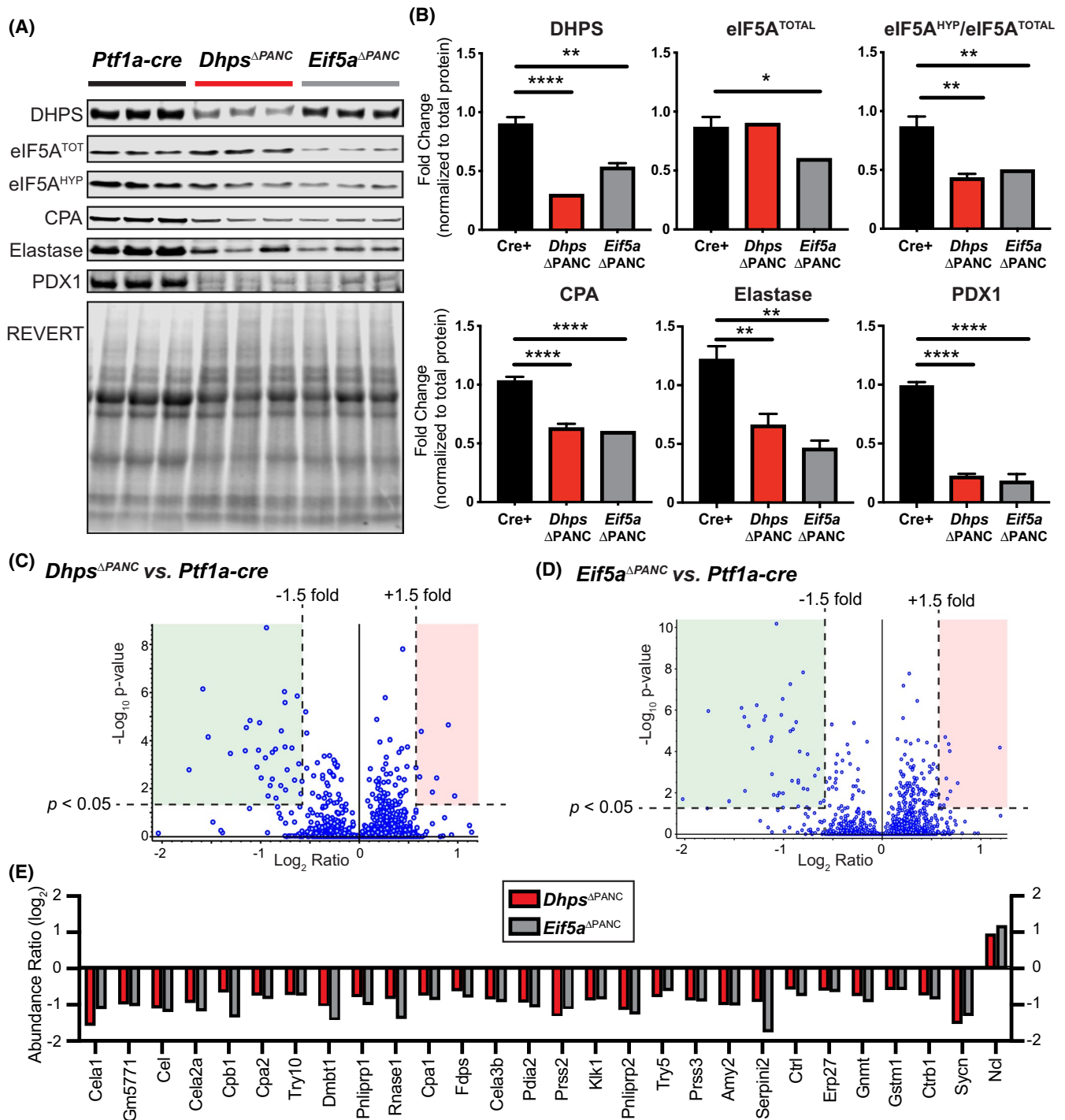


FIGURE 6 The expression of proteins required for exocrine development and function are significantly altered in the absence of hypusine biosynthesis. A, Western blot analysis of E18.5 pancreata harvested from *Ptf1a-cre* (control), *Dhps*^{ΔPANC}, and *Eif5a*^{ΔPANC} mice. DHPS, total eIF5A (eIF5A^{TOT}), hypusinated eIF5A (eIF5A^{HYP}), CPA, Elastase, and Pdx1 expression was measured. B, Densitometry values were normalized to total protein input as detected by Revert. Relative protein expression levels are shown in the bar graphs. Data are presented as mean ± SEM, n = 3/group. **P* < .05, ***P* < .005, *****P* < .0001. C,D, Volcano plots displaying proteomic data from the *Dhps*^{ΔPANC} or *Eif5a*^{ΔPANC} mutants compared with *Ptf1a-cre* controls. Each dot represents a protein; those in the shaded areas were identified as significantly up- (red) and down- (green) regulated in the mutants with a minimum fold change of 1.5 and *P* < .05. E, Proteins identified as differentially expressed in both the *Dhps*^{ΔPANC} and *Eif5a*^{ΔPANC} compared with the *Ptf1a-cre* control

could represent a curative therapy for these diseases. In this study, we identified that hypusine biosynthesis is critical for exocrine pancreas development. Moreover, we have shown

that genetic deletion of *Dhps* in the pancreas results in altered mRNA translation and reduced protein synthesis, including a specific reduction in the synthesis of digestive enzymes and

proteins that influence cellular development. Together these data identify a pathway that could be exploited for exocrine pancreas regeneration.

Given that both DHPS and eIF5A are essential for life, examining the impact on mammalian pancreas development requires animal models with cell type-specific genetic deletions. Our *Dhps*^{ΔPANC} and *Eif5a*^{ΔPANC} mutant mice are such models; however, assessing the full effect of the resultant protein loss can prove technically challenging. The decrease in DHPS (Figures 1, 5, and 6) and eIF5A (Figure 6) that we quantified was not as dramatic as expected given the observed phenotype and the robust *Ptf1a-cre* driver used to generate these mouse models, which illustrates the technical issue. The reduction in DHPS and eIF5A in the *Dhps*^{ΔPANC} and *Eif5a*^{ΔPANC} mutant pancreata, respectively, quantified by immunoblot were likely not the most accurate reflection of the true loss of either protein in these knockout pancreata given that the lysate evaluated was from whole tissue. Whole pancreas tissue contains many cell types including epithelial, mesenchymal, and endothelial cells. *Ptf1a* (the cre driver) is not expressed in the mesenchyme or endothelial cells and therefore the lysates evaluated by immunoblot were of a mixed population of cells that included those with and without cre expression and therefore with and without *Dhps* or *Eif5a* genetic deletion. Thus, the true reduction of DHPS or eIF5A in the pancreatic epithelium was likely greater than shown by our quantitative immunoblots. In line with this, the in situ hybridization presented in Figure S1, which we used to confirm *Eif5a* gene deletion when using our new *Eif5a* conditional allele, showed significant loss of gene expression in the pancreas of this mouse model.

Similar to the quantification of DHPS and eIF5A protein expression, the best available technique to measure the amount of hypusinated eIF5A (eIF5A^{HYP}) present in dissected tissues is immunoblot, using an antibody that recognizes the hypusine residue.²³ We utilized this method; however, as stated above, quantifying protein expression in the pancreas of our conditional mutants does come with the caveat that the lysate made from dissected pancreas represents a mixed population of deleted and not-deleted cells. Whereas our data show a significant reduction in eIF5A^{HYP} in both the *Dhps*^{ΔPANC} and *Eif5a*^{ΔPANC} mutants, this may represent an underestimate of the reduction in eIF5A^{HYP} in the pancreas.

Notably, our mouse models of *Dhps* and *Eif5a* deletion in the pancreas confirm that these genes are not required for endocrine cell development. Data presented in Figure S3 confirmed expression of *Dhps* and *Eif5a* in cell populations in the epithelium of the developing embryonic pancreas that become both endocrine and exocrine. Moreover, our previously published work identified expression in endocrine and exocrine cells in the adult pancreas of mouse and human.³³ However even with the expression of DHPS and eIF5A in endocrine cells in both of our mutant mouse models, the islets

were spared despite massive exocrine pancreas loss. Thus, our studies demonstrate that hypusine biosynthesis is dispensable for islet cell development, and confirm that the improved outcomes on diabetes observed after pharmacological inhibition of DHPS in non-obese diabetic (NOD) mice³⁴ was likely due to reduced DHPS function in the inflammatory cells rather than a direct effect on the beta cells. Interestingly, recent studies addressing the role of DHPS in the postnatal beta cell have revealed a function for this enzyme in the expansion of beta cell mass in response to insulin resistance.¹⁸ Therefore, it is clear that DHPS functions both in the embryonic and postnatal pancreas; however, the role in cellular growth and development in the islet appears context dependent. Our ongoing studies are addressing this complexity and will assist in understanding the role of hypusine biosynthesis in the developing islet and beta cell.

Another open question related to hypusinated eIF5A and its contribution to cellular growth and development is the role it plays in the setting of ER stress. Published studies have presented contrasting data wherein loss or inhibition of eIF5A^{HYP} can both perpetuate and alleviate ER stress.^{35,36} Given that ER stress can also result in cell death/apoptosis, and some mouse models where ER stress-related genes are mutated show effects in both the endocrine and exocrine pancreas,^{37,38} further examination of the contribution of cell death and ER stress to the pancreatic phenotype of our mutants is required.

Studies of cadaveric pancreas tissue from organ donors with type 1 diabetes (T1D) have revealed that exocrine pancreas volume is significantly reduced with duration of disease.³⁹ Moreover, reductions in exocrine-derived enzymes are observed in T1D.⁴⁰ It can be assumed that in a diseased state where endocrine or exocrine volume are altered, the crosstalk between these cell types will also be influenced. Interestingly, only a percentage of individuals with diseases characterized by exocrine pancreas loss and/or dysfunction, such as pancreatitis, exocrine insufficiency, and cystic fibrosis, will eventually present with endocrine dysfunction/diabetes.^{8,41-44} Understanding the molecular and cellular events that trigger certain individuals to progress to diabetes or that spare other individuals from endocrine dysfunction is needed. Our *Dhps*^{ΔPANC} and *Eif5a*^{ΔPANC} mutants provide a unique opportunity to investigate the contribution of acinar cells to exocrine-endocrine crosstalk.

To that end, our data provide evidence that DHPS and therefore eIF5A^{HYP} are required for the translation of multiple digestive enzymes. In particular, our immunoblot and unbiased quantitative proteomics data confirmed that the expression of the enzymes carboxypeptidaseA and elastase is significantly reduced in the absence of DHPS. These data raise the question of whether stimulating DHPS expression in acinar cells could force the expression of digestive enzymes and thus, provide a potential therapeutic avenue for treating

exocrine-deficient diseases. This would be an exciting application of our findings, but further investigation is needed.

More information is also required to completely understand the role of hypusinated eIF5A in all organ systems. In particular, determining why loss of hypusine biosynthesis may have specific effects on certain tissues/cell types and not others remain unknown. Published studies have shown that eIF5A^{HYP} may be required to facilitate the translation of iterated proline sequences that stall the ribosome.⁴⁵ Whereas this was clearly shown in yeast, the requirement for eIF5A^{HYP} to assist with the translation of poly-proline encoded stretches of sequence has not been confirmed in mammalian systems. In fact, it is more likely that in mammalian cells there exist a multitude of challenging sequences that require eIF5A^{HYP} to aid in or increase the rate of translation. Our work identified new targets in the developing pancreas that require eIF5A^{HYP} for translation; however, we expect these targets will not be the same in other organs. In fact, the recently identified human monogenic disease DHPS Deficiency,⁴⁶ which results from compound mutations in *DHPS*, demonstrates that each organ may have a different sensitivity to reductions in the amount of DHPS, and therefore the activity of eIF5A^{HYP}. A complete understanding of how eIF5A^{HYP} functions to facilitate mRNA translation in different organs, or as development proceeds, or in the context of cellular stress, remain open questions in the field.

ACKNOWLEDGMENTS

The authors would like to thank Drs. Amber Mosley and AJ Baucum for assistance with planning proteomic analyses, as well as Drs. Nicolas Berbari, Benjamin Perrin and Lata Balakrishnan for thoughtful discussions and use of imaging facilities in the IUPUI Department of Biology. This work was supported by funding from a Juvenile Diabetes Research Foundation (JDRF) Career Development Award (5-CDA-2016-194-A-N) and an NIH R01 (1R01DK121987-01A1) to TLM.

CONFLICT OF INTEREST

The authors declare that the research was conducted in the absence of any commercial or financial relationships that could be construed as a potential conflict of interest.

AUTHOR CONTRIBUTIONS

T. Mastracci and R. Mirmira designed the research; L. Padgett, M. Robertson, E. Anderson-Baucum, C. Connors, and T. Mastracci performed the research; L. Padgett, M. Robertson, E. Anderson-Baucum, W. Wu, R. Mirmira and T. Mastracci analyzed data; L. Padgett and T. Mastracci wrote the paper. All authors edited and approved the final draft of the manuscript.

ORCID

Teresa L. Mastracci  <https://orcid.org/0000-0003-1956-1951>

REFERENCES

- Pan FC, Wright C. Pancreas organogenesis: from bud to plexus to gland. *Dev Dyn*. 2011;240(3):530-565.
- Sambathkumar R, Migliorini A, Nostro MC. Pluripotent stem cell-derived pancreatic progenitors and β -like cells for type 1 diabetes treatment. *Physiology (Bethesda)*. 2018;33(6):394-402.
- Nair GG, Liu JS, Russ HA, et al. Recapitulating endocrine cell clustering in culture promotes maturation of human stem-cell-derived β cells. *Nat Cell Biol*. 2019;21(2):263-274.
- Castro-Gutierrez R, Michels AW, Russ HA. β Cell replacement: improving on the design. *Curr Opin Endocrinol Diabetes Obes*. 2018;25(4):251-257.
- Sneddon JB, Tang Q, Stock P, et al. Stem cell therapies for treating diabetes: progress and remaining challenges. *Cell Stem Cell*. 2018;22(6):810-823.
- Accili D, Talchai SC, Kim-Muller JY, et al. When β -cells fail: lessons from dedifferentiation. *Diabetes Obes Metab*. 2016;18(Suppl 1):117-122.
- Dominguez-Muñoz JE. Diagnosis and treatment of pancreatic exocrine insufficiency. *Curr Opin Gastroenterol*. 2018;34(5):349-354.
- Uc A, Andersen DK, Bellin MD, et al. Chronic pancreatitis in the 21st century—research challenges and opportunities. *Pancreas*. 2016;45(10):1365-1375.
- Gutierrez E, Shin BS, Woolstenhulme CJ, et al. eIF5A promotes translation of polyproline motifs. *Mol Cell*. 2013;51(1):35-45.
- Saini P, Eyler DE, Green R, Dever TE. Hypusine-containing protein eIF5A promotes translation elongation. *Nature*. 2009;459(7243):118-121.
- Schuller AP, Wu CC-C, Dever TE, Buskirk AR, Green R. eIF5A functions globally in translation elongation and termination. *Mol Cell*. 2017;66(2):194-205.e5.
- Park MH, Cooper HL, Folk JE. Identification of hypusine, an unusual amino acid, in a protein from human lymphocytes and of spermidine as its biosynthetic precursor. *Proc Natl Acad Sci U S A*. 1981;78(5):2869-2873.
- Park MH. The post-translational synthesis of a polyamine-derived amino acid, hypusine, in the eukaryotic translation initiation factor 5A (eIF5A). *J Biochem*. 2006;139(2):161-169.
- Wolff EC, Kang KR, Kim YS, Park MH. Posttranslational synthesis of hypusine: evolutionary progression and specificity of the hypusine modification. *Amino Acids*. 2007;33(2):341-350.
- Mastracci TL, Robertson MA, Mirmira RG, Anderson RM. Polyamine biosynthesis is critical for growth and differentiation of the pancreas. *Sci Rep*. 2015;24(5):13269.
- Templin AT, Maier B, Nishiki Y, Tersey SA, Mirmira RG. Deoxyhypusine synthase haploinsufficiency attenuates acute cytokine signaling. *Cell Cycle*. 2011;10(7):1043-1049.
- Nishimura K, Lee SB, Park JH, Park MH. Essential role of eIF5A-1 and deoxyhypusine synthase in mouse embryonic development. *Amino Acids*. 2012;42(2-3):703-710.
- Levasseur EM, Yamada K, Piñeros AR, et al. Hypusine biosynthesis in β cells links polyamine metabolism to facultative cellular proliferation to maintain glucose homeostasis. *Sci Signal*. 2019;12(610). <https://doi.org/10.1126/scisignal.aax0715>
- Kawaguchi Y, Cooper B, Gannon M, Ray M, MacDonald RJ, Wright CV. The role of the transcriptional regulator Ptf1a in converting intestinal to pancreatic progenitors. *Nat Genet*. 2002;32(1):128-134.

20. Madisen L, Zwingman TA, Sunkin SM, et al. A robust and high-throughput Cre reporting and characterization system for the whole mouse brain. *Nat Neurosci.* 2010;13(1):133-140.
21. Chao CS, Loomis ZL, Lee JE, Sussel L. Genetic identification of a novel NeuroD1 function in the early differentiation of islet alpha, PP and epsilon cells. *Dev Biol.* 2007;312(2):523-532.
22. Mastracci TL, Anderson KR, Papizan JB, Sussel L. Regulation of NeuroD1 contributes to the lineage potential of Neurogenin3+ endocrine precursor cells in the pancreas. *PLoS Genet.* 2013;9(2):e1003278.
23. Nishiki Y, Farb TB, Friedrich J, Bokvist K, Mirmira RG, Maier B. Characterization of a novel polyclonal anti-hypusine antibody. *Springerplus.* 2013;2:421.
24. Hatanaka M, Maier B, Sims EK, et al. Palmitate induces mRNA translation and increases ER protein load in Islet β -cells via activation of the mammalian target of rapamycin pathway. *Diabetes.* 2014;63(10):3404-3415.
25. Smith-Kinnaman WR, Berna MJ, Hunter GO, et al. The interactome of the atypical phosphatase Rtr1 in *Saccharomyces cerevisiae*. *Mol Biosyst.* 2014;10(7):1730-1741.
26. Mosley AL, Sardi ME, Pattenden SG, Workman JL, Florens L, Washburn MP. Highly reproducible label free quantitative proteomic analysis of RNA polymerase complexes. *Mol Cell Proteomics.* 2011;10(2):M110.000687.
27. Cleveland MH, Sawyer JM, Afelik S, Jensen J, Leach SD. Exocrine ontogenies: on the development of pancreatic acinar, ductal and centroacinar cells. *Semin Cell Dev Biol.* 2012;23(6):711-719.
28. Nishimura K, Murozumi K, Shirahata A, Park MH, Kashiwagi K, Igarashi K. Independent roles of eIF5A and polyamines in cell proliferation. *Biochem J.* 2005;385(Pt 3):779-785.
29. Torrelío BM, Paz MA, Gallop PM. The formation and stability of the hypusine containing protein in Chinese hamster ovary cells. *Biochem Biophys Res Commun.* 1987;145(3):1335-1341.
30. Bergeron RJ, Weimar WR, Müller R, et al. Effect of polyamine analogues on hypusine content in JURKAT T-cells. *J Med Chem.* 1998;41(20):3901-3908.
31. Hale MA, Kagami H, Shi L, et al. The homeodomain protein PDX1 is required at mid-pancreatic development for the formation of the exocrine pancreas. *Dev Biol.* 2005;286(1):225-237.
32. Tenner S, Baillie J, DeWitt J, Vege SS; American College of Gastroenterology. American College of Gastroenterology guideline: management of acute pancreatitis. *Am J Gastroenterol.* 2013;108(9):1400-15; 1416.
33. Mastracci TL, Colvin SC, Padgett LR, Mirmira RG. Hypusinated eIF5A is expressed in the pancreas and spleen of individuals with type 1 and type 2 diabetes. *PLoS ONE.* 2020;15(3):e0230627.
34. Colvin SC, Maier B, Morris DL, Tersey SA, Mirmira RG. Deoxyhypusine synthase promotes differentiation and proliferation of T helper type 1 (Th1) cells in autoimmune diabetes. *J Biol Chem.* 2013;288(51):36226-36235.
35. Robbins RD, Tersey SA, Ogihara T, et al. Inhibition of deoxyhypusine synthase enhances islet {beta} cell function and survival in the setting of endoplasmic reticulum stress and type 2 diabetes. *J Biol Chem.* 2010;285(51):39943-39952.
36. Mandal A, Mandal S, Park MH. Global quantitative proteomics reveal up-regulation of endoplasmic reticulum stress response proteins upon depletion of eIF5A in HeLa cells. *Sci Rep.* 2016;16(6):25795.
37. Lee A-H, Chu GC, Iwakoshi NN, Glimcher LH. XBP-1 is required for biogenesis of cellular secretory machinery of exocrine glands. *EMBO J.* 2005;24(24):4368-4380.
38. Harding HP, Zeng H, Zhang Y, et al. Diabetes mellitus and exocrine pancreatic dysfunction in perk-/- mice reveals a role for translational control in secretory cell survival. *Mol Cell.* 2001;7(6):1153-1163.
39. Campbell-Thompson M, Rodriguez-Calvo T, Battaglia M. Abnormalities of the exocrine pancreas in type 1 diabetes. *Curr Diab Rep.* 2015;15(10):79.
40. Li X, Campbell-Thompson M, Wasserfall CH, et al. Serum trypsinogen levels in type 1 diabetes. *Diabetes Care.* 2017;40(4):577-582.
41. Hart PA, Bellin MD, Andersen DK, et al. Type 3c (pancreatogenic) diabetes mellitus secondary to chronic pancreatitis and pancreatic cancer. *Lancet Gastroenterol Hepatol.* 2016;1(3):226-237.
42. Olesen HV, Drevinek P, Gulmans VA, et al. Cystic fibrosis related diabetes in Europe: Prevalence, risk factors and outcome; Olesen et al. *J Cyst Fibros.* 2020;19:321-327.
43. Das SLM, Singh PP, Phillips ARJ, Murphy R, Windsor JA, Petrov MS. Newly diagnosed diabetes mellitus after acute pancreatitis: a systematic review and meta-analysis. *Gut.* 2014;63(5):818-831.
44. Raman VS, Loar RW, Renukuntla VS, et al. Hyperglycemia and diabetes mellitus in children with pancreatitis. *J Pediatr.* 2011;158(4):612-616.e1.
45. Ude S, Lassak J, Starosta AL, Kraxenberger T, Wilson DN, Jung K. Translation elongation factor EF-P alleviates ribosome stalling at polyproline stretches. *Science.* 2013;339(6115):82-85.
46. Ganapathi M, Padgett LR, Yamada K, et al. Recessive rare variants in deoxyhypusine synthase, an enzyme involved in the synthesis of hypusine, are associated with a neurodevelopmental disorder. *Am J Hum Genet.* 2019;104(2):287-298.

SUPPORTING INFORMATION

Additional Supporting Information may be found online in the Supporting Information section.

How to cite this article: Padgett LR, Robertson MA, Anderson-Baucum EK, et al. Deoxyhypusine synthase, an essential enzyme for hypusine biosynthesis, is required for proper exocrine pancreas development. *The FASEB Journal.* 2021;35:e21473. <https://doi.org/10.1096/fj.201903177R>